CHEMISTRY & SUSTAINABILITY

CHEMSUSCHEM

ENERGY & MATERIALS

Supporting Information

Biochemical Capacitance of *Geobacter Sulfurreducens* Biofilms

Paulo R. Bueno,*[a] Germán D. Schrott,[b] Pablo S. Bonanni,[b] Silvia N. Simison,[b] and Juan P. Busalmen[b]

cssc_201403443_sm_miscellaneous_information.pdf

S.1. Geobacter Biofilm electrical model

Typically, electricity production by *Geobacter* biofilms is continuum if cells respiration is not disrupted by electrode depolarization, but it is to note indeed that biofilm cells are able of respiration at a certain level even after electrode fully depolarization, a fact attributed to electron storage in the haem groups of the vast amount of exocytoplasmic cytochromes found in this bacterial strain.[1]

Since pioneer works, DC current electrochemical techniques have been particularly useful in exploring potential dependent properties of *Geobacter* biofilms.[2] The approach, identified as Electrochemical Capacitance Spectroscopy (ECS)[3], a method derived from Electrochemical Impedance Spectrocopy (EIS), is particularly useful in analyzing electron transfer kinetics and redox density of states in molecular scale and redox confined films, and we use it here for the first time to analyze the *Geobacter* biofilm/electrode interface. Between DC techniques, the cyclic voltammetry has been by far the most informative one by showing the gating effect of cytochromes in electricity production and the oxidative catalysis feature of the microbial colony over acetate consumption[4]. Complementary, chronoamperometry in combination with numerical modeling have provided insights into charge accumulation inside biofilms,[1b] while gate measurements and light spectroscopy techniques have been cooperative in confirming the existence of potential driven redox gradients across their thickness.[5] AC current techniques on the other hand, have the potential to inform about frequency dependent properties of the biofilm/electrode interface, but most of this potential remains unexploited, since only a few works[6] have explored the use of EIS, providing estimations of biofilm capacitive and/or conductive elements properties, without integrating the whole electrochemical response of biofilms in a single model. A step forward in the analysis of impedance spectroscopy data is through its phasorial conversion to complex capacitance data.[3a, 7] In doing this, problems related to potential dependence in the behavior of charge transfer (resistance) and charge accumulation (capacity) processes are readily resolved.[3a, 7]

For biofilms grown under fuel saturation as in the case here, the porous model can be simplified as a transmission line of just one conductive channel (Z_c in Figure 1*b*) and the general impedance of the system is then appropriately given by:

$$Z = \lambda Z_c \coth(L/\lambda), \qquad (1)$$

where $\lambda = (\zeta_c/Z_c)^{1/2}$, with ζ_c representing the impedance of each individual cell (Figure 1*b*) and where *L* is the active thickness of the biofilm (typically around 50 μm).[8] ζ_c can be divided into equivalent circuit terms named

R_{ct}, C_r and R_t, as in the parallel and series configuration shown in Figure 1*c*. R_{ct} is a charge transfer resistance ($R_{ct} = r_{ct}L$) while C_r is an electrochemical or redox capacitance ($C_r = c_rL$); both in series represent the balance of energy (loss and storage, respectively) during the microbial individual activity in metabolizing the electron source and are parallel to $R_t = r_tL$, a recombination resistance that acts as a shunt to the R_{ct} and C_r serial process. It may be noted that differing from the classical picture, the electrochemical meaning and mechanical statistic description of these circuit elements are here as function of the electrochemical potential and in turn, of the biofilm energy state or respiratory level, thus appropriately representing potential gradients existing inside biofilms[5]).

It is important to highlight that in spite of impedance parameters involved in Eqn. (1), in the present work we focus only on the physical/physiological meaning of C_r. This capacitive feature of the presented model can be obtained by fitting impedance spectral data to Eqn. (1), or either more easily by graphical analysis of capacitive Bode diagrams at lower frequency, as exemplified in Figs. S1*b* and S1*c* (see details below and in S2 section on how to construct such ECS diagrams from EIS data). In the limit of lower frequency (i.e. when the electron states at electrode are in equilibrium to those of redox exocytoplastic cytochromes) the respiration process is entirely controlled by the energy involved with C_r. Accordingly, C_r is the truly relevant parameter to thermodynamic model discussed in the main text. In controllably moving electrode potential to different energetic levels, but keeping the equilibrium between them and those redox levels (or respiration level) associated with C_r, we observe that a Boltzmann statistics is obeyed. In summary, although impedance/capacitance spectroscopy analysis were key to identify the physical/physiological meaning and potential dependence of C_r in the context of electrogenic *Geobacter* biofilms, once C_r function is known (Eqn. 6 in the main text), it can be either and easily investigated and quantified performing voltammetric or chronoamperometric methods. In physical chemistry terms, C_r is not the classical or electrostatic (geometric) capacitance, as frequently used in impedance modelling studies by following the general knowledge, but instead it is an electron chemical capacitance[9] that has a dependence with electrode potential (see Eqns. 5 and 6). C_r energetic donor/acceptor states are associated with reduced and oxidized chemical states[9-10] in the biofilm, which arise specifically from the coupling of a supporting electrode density of states to the redox sites molecular density of states.

In *Geobacter* biofilms operating in their maximum current performance, capacitive contribution dominates the electron transfer process and negligible (or none) *dc* current is present (Figure S2*a*). It is resolved experimentally by EIS analysis as shown in Figure S1*a*, where typical Nyquist diagrams reveal the absence of an effective *dc* conductivity (when scanned or perturbed externally) at lower frequencies. This response is appropriately modelled in the equivalent circuit presented here by R_t (as to be detailed elsewhere) that acts as

an ideal isolator (i.e., $R_t \rightarrow \infty$) in the maximum respiratory level of the biofilm, thus hiding external access from the electrode to biofilm internal faradaic process. As clearly shown by results presented in Figure S1*b*, ECS has advantages over traditional EIS in specifically detecting C_r, revealing the coupling between the electrode and cytochrome redox sites in the biofilm.[3, 7] As external cytochromes are the natural electron sink for the respiratory process, ECS thus offers an unprecedented opportunity to explore for the first time and noninvasively the energetic internal path of the bacterial cell machinery, indeed revealing the cost of biological energy conservation (see main text).

According to the model presented here (Figure 1*c*) the internal charge transfer resistance associated to C_r is R_{ct} , both representing a typical redox process that, operating on the microbial colony in isolation from the external perturbation, may be energetically feed internally (in terms of electrochemical driving force) by the work performed by the colony on available (bio)chemical energy. In this context, R_{ct} is viewed as a measure of the average energy loss of the bioenergetic process, i.e. as the electric analogue of the biological energy spent during the respiration process exclusively related to transfer internalized electrons to exocytoplasmatic cytochromes (note the energy lost in the electron transport outside exocytoplasmatic membranes to electrode is though not contained on this term).

As previously stated, C_r is the energy storage element of ζ_c and is of particular importance for the analysis of electrogenic biofilms, because of this energetic particular feature. The capacitive effects on kinetics is found at intermediate to lower frequencies (from 10 Hz to 5 mHz) in EIS/ECS diagrams (Figure S1), from which a time scale of ~ 10 s can be obtained as $\tau = R_{ct}C_r$ (see Figure S1*d*), for the occupancy process of redox (cytochrome) centres. τ thus can inform on the rate at which chemical energy is converted into electricity by the bacterial population.

S2. Experimental method

Biofilms of *Geobacter sulfurreducens* were grown into continuous mode at 32 °C within a 100 cm^3 stirred electrochemical cell. A graphite disk with a diameter of 0.4 cm was used as the working electrode. Before use, the electrode surface was polished with 1000 grade silicon carbide paper and sonicated three times in distilled water. The electrode potential steady state potential for EIS was set against Ag|AgCl – 3M NaCl reference electrode. Platinum wire was used as the counter electrode.

A culture medium lacking electron acceptors and containing sodium bicarbonate (100 mM) and acetate (20 mM) as the carbon source was prepared as described in literature[1b, 11]. It was circulated by the electrochemical reactor using biocompatible Pharma pure tubings (Saint Gobain, OH, USA) and a low rate peristaltic pump

(BT100 – 2J, Longerpump, USA). The pH of the medium was kept constant of 7.3 by bubbling all media reservoirs and the reactor with a mixture of N_2/CO_2 (80:20). The gas mixture was filtered through a Variant C553120 oxygen filter to eliminate oxygen traces. All the electrochemical assays were performed using an Autolab PGSTAT101 potentiostat controlled by Nova 1.6-dedicated software. All experiments were performed when the biofilms reached the stationary growth phase, which was approximately 8-9 days after inoculation. Final current densities were in all cases approximately 7 A m^{-2}.

AC frequencies ranged from 0.1 MHz to 10 mHz with an amplitude of 10 mV peak to peak were employed for EIS analysis. All the obtained impedance data were checked regarding compliance with the constraints of linear systems theory by Kramers-Kronig using the appropriate routine of the FRA AUTOLAB software. The complex $Z^*(\omega)$ (impedance) function can be converted into $C^*(\omega)$ (capacitance) by $C^*(\omega) = 1/i\omega Z^*(\omega)$, where ω is the angular frequency and $i = \sqrt{-1}$ (i.e., complex number). Practically, this involves taking the data resolved in a standard impedance analysis [$Z^*(\omega)$], sampled across a range of frequencies at any steady-state potential, and converting it phasorially into complex capacitance [$C^*(\omega)$] with its real and imaginary components. In processing $Z^*(\omega)$ datasets in this way one obtains the imaginary part of the capacitance by noting that $C'' = \varphi Z'$ and $C' = \varphi Z''$, where $\varphi = (\omega|Z|^2)^{-1}$ and $|Z|$ is the modulus of Z^*.

S3. Cyclic Voltammetry (CV) and Electrochemical Capacitance Spectroscopy (ECS) curves obtained at different respiration levels

The ECS and EIS approaches are comparatively analysed in Figures S1 and S2. ECS has advantages over traditional electrochemical impedimetric approach in revealing faradaic processes when capacitive contribution dominates the electron transfer process and negligible (or none) *dc* current is present (see Figure S1), which is the case of maximum respiration level of the *Geobacter* biofilm. Accordingly, Figure S1*a* shows typical Nyquist impedance diagrams of biofilm where the absence of an effective *dc* conductivity (when scanned or perturbed externally) is evident at lower frequency, meanwhile ECS diagrams (Figure S1*b*) additionally reveal the internal charge transfer resistance associated with charging/discharging of C_r term (effectively acting as the conductive internal path – where the redox current flows – of the cell machinery associated with the energy whose origin resides on the work done by the biofilm through its intrinsic biochemistry energy). The ECS and EIS are equally important to evaluate the variation of the equivalent circuit model during electrode polarization as shown in Figure S2. The experimental curves and spectra in Figures S1 are always compared with theoretical model (as fitted and visualized in blue line in Figure S1) developed and explained in the main text. The inverse dependence

with potential of the shunt resistance with respect of redox capacitance is better visualized in comparing Figure S2*b* and S2*c*. The analysis of the resistance terms and kinetics involved will be published elsewhere.

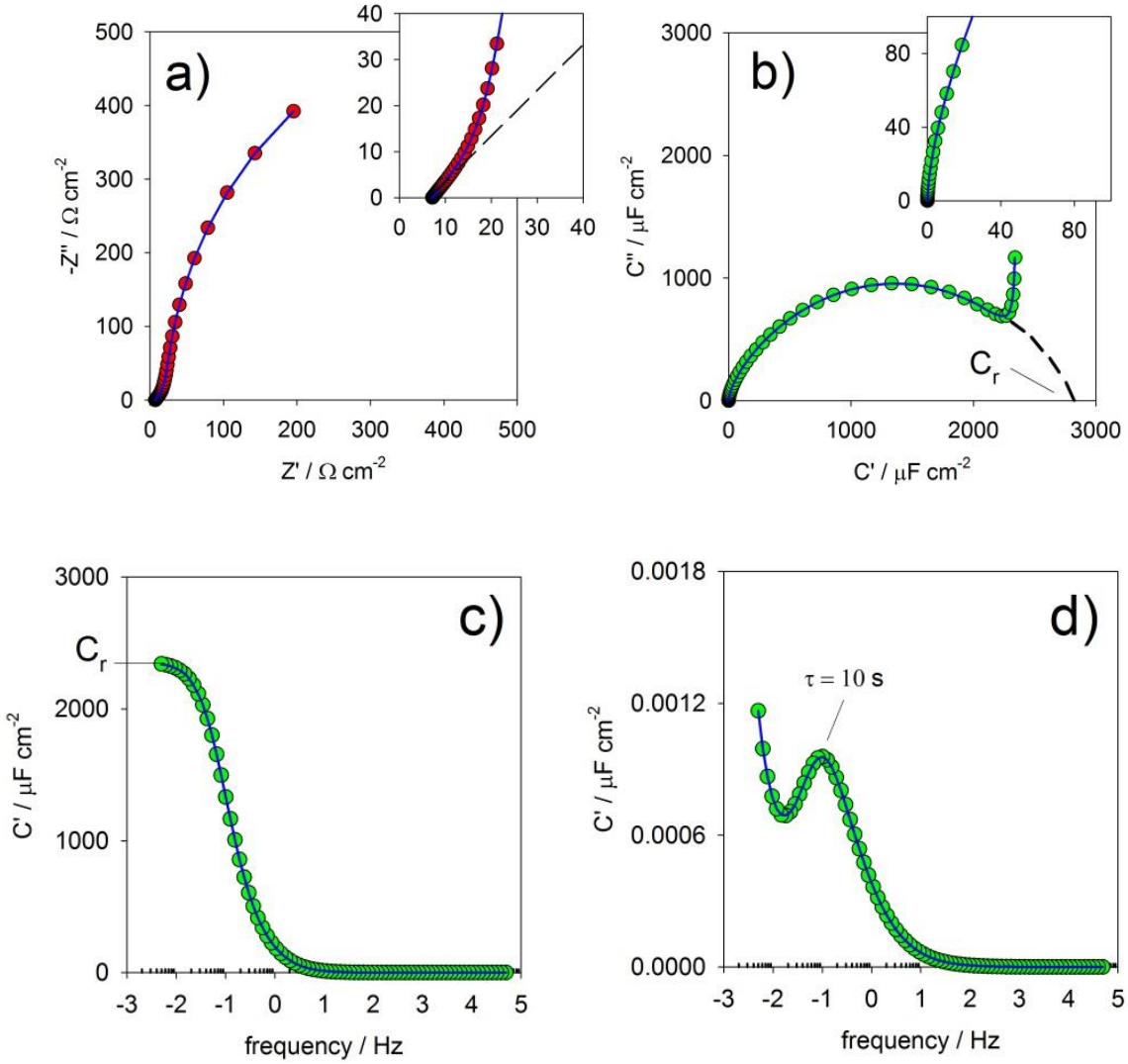

Figure S1. a) The impedance diagram of microbial biofilm at 50 mV with respect to Ag|AgCl, i.e. at the maximum current delivered to the external circuit (maximum microbial respiratory activity). The inset depicts the high frequency region in which the slope dashed line comprising a 45 degree demonstrates the porous/transport behavior of the electron conduction into cytochrome chains (observe the minimum series conductance). The diagram shows a capacitive behavior that is resolved by ECS approach in b). From both b) and c) diagrams the value of C_r is easily obtained as well as the time scale of the associated redox process as indicated in d), $\tau = R_{ct}C_r \sim 10$ s. Blue line is the fitting to theoretical model.

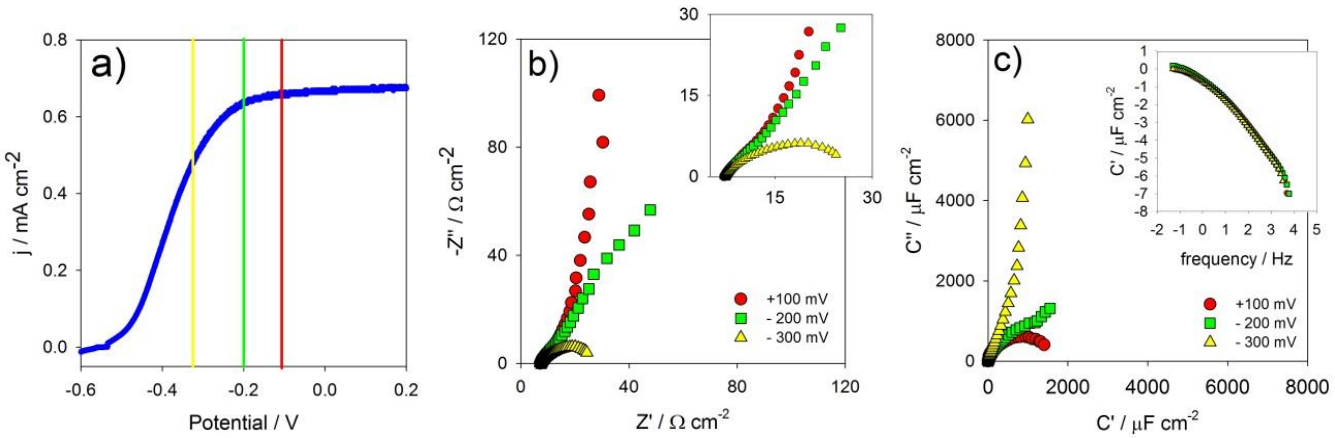

Figure S2. a) Current density *versus* potential curve for a MFC under equilibrium scan rate of 1 mV s^{-1} obtained for a Biofilm thickness larger than 60 µm. The colouring lines are highlighting the potentials of +100 mV (red), -200 mV (green) and -300 mV (red). As lower the potential lower is the biofilm respiratory rate. b) The corresponding Nyquist impedimetric diagrams of highlighted potentials of Figure 3*a* demonstrate the effect in lowering the respiratory rate. Ultimately this is monitored by changes on R_t within the exchange impedance term of the transmission line. The meaning of R_t is stated in the main text and it can be noted that as higher the respiration rate higher is the magnitude of R_t. c) Nyquist capacitive diagrams of highlighted potentials of Figure 3*a*. Equivalently to b) as higher is the respiration rate higher is the capacitive behavior (higher the magnitude of R_t term).

References

[1] aG. D. Schrott, P. S. Bonanni, L. Robuschi, A. Esteve-Nuñez, J. P. Busalmen, *Electrochimica Acta* **2011**, *56*, 10791-10795; bP. Sebastian Bonanni, G. D. Schrott, L. Robuschi, J. P. Busalmen, *Energy & Environmental Science* **2012**, *5*, 6188-6195; cN. S. Malvankar, T. Mester, M. T. Tuominen, D. R. Lovley, *Chemphyschem* **2012**, *13*, 463-468; dA. Esteve-Nunez, J. Sosnik, P. Visconti, D. R. Lovley, *Environ. Microbiol.* **2008**, *10*, 497-505.

[2] aK. Fricke, F. Harnisch, U. Schroder, *Energy & Environmental Science* **2008**, *1*, 144-147; bE. Marsili, J. B. Rollefson, D. B. Baron, R. M. Hozalski, D. R. Bond, *Applied and Environmental Microbiology* **2008**, *74*, 7329-7337.

[3] aP. R. Bueno, J. J. Davis, G. Mizzon, *J. Phys. Chem. C* **2012**, *116*, 8822–8829; bP. R. Bueno, D. Gimenez-Romero, F. F. Ferreira, G. O. Setti, *Electrochimica Acta* **2010**, *55*, 6147-6155.

[4] E. Marsili, J. Sun, D. R. Bond, *Electroanalysis* **2010**, *22*, 865-874.

[5] aL. Robuschi, J. Pablo Tomba, G. D. Schrott, P. Sebastian Bonanni, P. Mariela Desimone, J. Pablo Busalmen, *Angewandte Chemie-International Edition* **2013**, *52*, 925-928; bR. M. Snider, S. M. Strycharz-Glaven, S. D. Tsoi, J. S. Erickson, L. M. Tender, *Proceedings of the National Academy of Sciences* **2012**, *109*, 15467-15472.

[6] aS. Srikanth, E. Marsili, M. C. Flickinger, D. R. Bond, *Biotechnology and Bioengineering* **2008**, *99*, 1065-1073; bN. S. Malvankar, M. T. Tuominen, D. R. Lovley, *Energy & Environmental Science* **2012**, *5*, 5790-5797; cJ. T. Babauta, H. Beyenal, *Biotechnology and Bioengineering* **2014**, *111*, 285-294; dA. ter Heijne, H. V. M. Hamelers, M. Saakes, C. J. N. Buisman, *Electrochimica Acta* **2008**, *53*, 5697-5703.

[7] P. R. Bueno, F. Fabregat-Santiago, J. J. Davis, *Anal. Chem.* **2012**, *85*, 411-417.

[8] D. R. Bond, S. M. Strycharz, L. Tender, C. I. Torres, *ChemSusChem* **2012**, *5*, 1099-1105.

[9] P. R. Bueno, G. T. Feliciano, J. J. Davis, *Phys. Chem. Chem. Phys.* **2015**.

[10] P. R. Bueno, J. J. Davis, *Analytical Chemistry* **2014**, *86*, 1337-1341.

[11] G. D. Schrott, P. Sebastian Bonanni, L. Robuschi, A. Esteve-Nunez, J. Pablo Busalmen, *Electrochimica Acta* **2011**, *56*, 10791-10795.